British Journal of Pharmacology (2007) 151, 655–665

0007–1188/07 $30.00
www.brjpharmacol.org

RESEARCH PAPER

Selective positive modulation of the SK3 and SK2 subtypes of small conductance Ca^{2+}-activated K^+ channels

C Hougaard, BL Eriksen, S Jørgensen, TH Johansen, T Dyhring, LS Madsen, D Strøbæk and P Christophersen

NeuroSearch A/S, Pederstrupvej 93, Ballerup, Denmark

Background and purpose: Positive modulators of small conductance Ca^{2+}-activated K^+ channels (SK1, SK2, and SK3) exert hyperpolarizing effects that influence the activity of excitable and non-excitable cells. The prototype compound 1-EBIO or the more potent compound NS309, do not distinguish between the SK subtypes and they also activate the related intermediate conductance Ca^{2+}-activated K^+ channel (IK). This paper demonstrates, for the first time, subtype-selective positive modulation of SK channels.
Experimental approach: Using patch clamp and fluorescence techniques we studied the effect of the compound cyclohexyl-[2-(3,5-dimethyl-pyrazol-1-yl)-6-methyl-pyrimidin-4-yl]-amine (CyPPA) on recombinant hSK1-3 and hIK channels expressed in HEK293 cells. CyPPA was also tested on SK3 and IK channels endogenously expressed in TE671 and HeLa cells.
Key results: CyPPA was found to be a positive modulator of hSK3 (EC_{50} = 5.6 ± 1.6 μM, efficacy 90 ± 1.8 %) and hSK2 (EC_{50} = 14 ± 4 μM, efficacy 71 ± 1.8 %) when measured in inside-out patch clamp experiments. CyPPA was inactive on both hSK1 and hIK channels. At hSK3 channels, CyPPA induced a concentration-dependent increase in the apparent Ca^{2+}-sensitivity of channel activation, changing the $EC_{50}(Ca^{2+})$ from 429 nM to 59 nM.
Conclusions and implications: As a pharmacological tool, CyPPA may be used in parallel with the IK/SK openers 1-EBIO and NS309 to distinguish SK3/SK2- from SK1/IK-mediated pharmacological responses. This is important for the SK2 and SK1 subtypes, since they have overlapping expression patterns in the neocortical and hippocampal regions, and for SK3 and IK channels, since they co-express in certain peripheral tissues.
British Journal of Pharmacology (2007) **151,** 655–665; doi:10.1038/sj.bjp.0707281; published online 8 May 2007

Keywords: SK channel; IK channel; gating; positive modulator; 1-EBIO; NS309; patch clamp; subtype-selective

Abbreviations: AHP, afterhyperpolarization; BK channel, large conductance Ca^{2+}-activated K^+ channel; BMB, bicuculline methobromide; BSA, bovine serum albumin; BTC-AM, benzothiazole coumarin acetoxymethyl ester; CAM, calmodulin; CAMBD, calmodulin-binding domain; ChTX, charybdotoxin; CyPPA, cyclohexyl-[2-(3,5-dimethyl-pyrazol-1-yl)-6-methyl-pyrimidin-4-yl]-amine; DC-EBIO, 5,6-dichloro-1-ethyl-1,3-dihydro-2H-benzimidazol-2-one; DMSO, dimethylsulphoxide; DRG, dorsal root ganglion; 1-EBIO, 1-ethyl-2-benzimidazolinone; FLIPR, fluorometric imaging plate reader; HEK, human embryonic kidney; hERG, human ether-a-go-go-related gene; h, human; I_{AHP}, afterhyperpolarizing current; IK channel, intermediate conductance Ca^{2+}-activated K^+ channel; *I-V*, current–voltage; NS309, 6,7-dichloro-1H-indole-2,3-dione 3-oxime; PBS, phosphate-buffered saline; SK channel, small conductance Ca^{2+}-activated K^+ channel.

Introduction

Small conductance Ca^{2+}-activated K^+ channels (SK channels) are important regulators of excitability, endogenous firing pattern and synaptic integration in many neurons (Bond *et al*., 2005). Three SK channel subtypes exist (SK1-3; Kohler *et al*., 1996) and are widely distributed in the central nervous system (CNS) (Stocker and Pedarzani, 2000) as well as in the periphery. SK channels and the peripherally expressed intermediate conductance Ca^{2+}-activated K^+ channel (IK; Ishii *et al*., 1997), constitute a molecular family of voltage-independent channels, that are gated by Ca^{2+} binding to calmodulin (CAM) tightly associated with a CAM-binding domain (CAMBD) in the C-terminal region (Xia *et al*., 1998; Khanna *et al*., 1999). Crystallographic data from C-terminal peptides of the SK2 channel indicate that dimers

Correspondence: Dr P Christophersen, NeuroSearch A/S, Pederstrupvej 93, DK 2750, Ballerup, Denmark.
E-mail: pc@neurosearch.dk
Received 28 December 2006; revised 20 March 2007; accepted 21 March 2007; published online 8 May 2007

of CAMBD associate with two CAM molecules, each binding 1 or 2 Ca^{2+} at the EF hand motifs 1 and 2 (Schumacher *et al*., 2001). The binding of Ca^{2+} is potent (effector concentration for half-maximum response (EC_{50}) $\approx$400 nM), highly co-operative ($n_H = 4–5$) and thought to involve binding of 4–8 Ca^{2+} in all the SK channel subtypes (Xia *et al*., 1998). In contrast, the intermediate conductance Ca^{2+}-activated K^+ channel (IK channel) exhibits a significantly lower Hill coefficient for Ca^{2+} activation (but identical EC_{50} value; Ishii *et al*., 1997), indicating that molecular differences exist between the gating mechanisms of SK and IK channels despite their overall similarity in Ca^{2+} binding.

Ca^{2+}-dependent activation of IK/SK channels is facilitated by certain small organic compounds. 1-Ethyl-2-benzimidazolinone (1-EBIO) was the first described positive modulator of IK channels (Devor *et al*., 1996; Jensen *et al*., 1998) and SK channels (Syme *et al*., 2000). 1-EBIO causes a leftward shift in the Ca^{2+}-activation curves for IK/SK channels (Pedersen *et al*., 1999; Pedarzani *et al*., 2001) and strongly reduces the rate of deactivation upon Ca^{2+} removal. The 1-EBIO interaction site has been localized close to the CAMBD in the C-terminal region (Pedarzani *et al*., 2001). In addition, the more potent 1-EBIO analogue, 5,6-dichloro-1-ethyl-1,3-dihydro-2H-benzimidazol-2-one (DC-EBIO) (Singh *et al*., 2001; Pedarzani *et al*., 2005), the centrally acting muscle relaxant drugs zoxazolamine and chlorzoxazone (Cao *et al*., 2001), as well as the neuroprotectant riluzole (Cao *et al*., 2002), all have IK/SK activating properties. 6,7-Dichloro-1H-indole-2,3-dione 3-oxime (NS309) is a recently described compound in this functional class and is orders of magnitude more potent than 1-EBIO (Strøbæk *et al*., 2004; Pedarzani *et al*., 2005). However, NS309 still exhibits the characteristic 1-EBIO-like selectivity for the IK/SK channels, being most potent on IK and 10–20 times less active on the SK subtypes.

Despite their lack of SK subtype selectivity, 1-EBIO and other positive modulators of IK/SK channels have been used to elucidate the role of SK channels in the regulation of neuronal excitability. For example debate continues as to the contribution of SK channels to hippocampal CA1 neuron spike frequency adaptation (Bond *et al*., 2004; Gu *et al*., 2005). The involvement of SK channels is strongly supported by the effects of 1-EBIO and NS309, which both increase the size and duration of the Ca^{2+}-activated afterhyperpolarizing current (I_{AHP}), increase the intermediate duration afterhyperpolarization (mAHP), augment spike frequency adaptation and reduce excitability following constant current stimuli (Pedarzani *et al*., 2001, 2005). Furthermore, the negative modulator (*R*)-*N*-(benzimidazol-2-yl)-1,2,3,4-tetrahydro-1-naphtylamine (NS8593), which decreases the apparent SK channel Ca^{2+} sensitivity, also reduces I_{AHP} (Strøbæk *et al*., 2006). Because the SK channel modulators exclusively affect Ca^{2+} sensitivity and have no effect on maximally activated SK channels, these results show that SK channels are not saturated with Ca^{2+} following action potentials or even long depolarizing stimuli. Therefore, these pharmacological agents indirectly demonstrate the possibility that modulation of SK channel Ca^{2+} sensitivity could be a sensitive endogenous mechanism for fine-tuning neuronal excitability. Importantly, it has also been shown that SK2 channel Ca^{2+} sensitivity can be decreased by phosphorylation of CAM threonine-80 via protein kinase CK2, and conversely increased by dephosphorylation via protein phosphatase 2A (Bildl *et al*., 2004). Therefore, SK channels may under some regulatory conditions, be too insensitive to intracellular Ca^{2+} to contribute significantly to spike frequency adaptation unless their Ca^{2+} sensitivity is increased by dephosphorylation or by the presence of a positive modulator of SK channels (Faber and Sah, 2002).

Subtype-selective SK channel modulators are clearly needed to assign specific SK channel subtypes to observed pharmacological responses. However, owing to the conserved gating mechanism within the IK/SK channel family and the identical activation curves for Ca^{2+} obtained with the SK1-3 channels (Xia *et al*., 1998), the identification of subtype-selective positive modulators has only been a hypothetic possibility. In this study we demonstrate that the compound, cyclohexyl-[2-(3,5-dimethyl-pyrazol-1-yl)-6-methyl-pyrimidin-4-yl]-amine (CyPPA) is a selective positive modulator of SK3 and SK2 channels exhibiting the following selectivity profile: hSK3 > hSK2 >> hSK1 (inactive) = hIK (inactive). The EC_{50} value of CyPPA on SK3 channels was 5.6 μM, which although higher than that of NS309 (0.3 μM), was lower than those of DC-EBIO (16 μM), 1-EBIO (1040 μM), and other available non selective SK activators.

Methods

Cell cultures

Establishment of human embryonic kidney (HEK) 293 cell lines expressing hSK1, hSK2, hSK3 and hIK channels has been described previously (Strøbæk *et al*., 2004). HeLa and TE671 cells were obtained from ATCC (Rockville, MD, USA). Cells were cultured in Dulbecco's modified Eagle's medium (DMEM; Cambrex BioScience, Verviers, Belgium) supplemented with 10% fetal calf serum (FCS; Sigma-Aldrich, Vallensbæk Strand, Denmark) at 37°C and 5% CO_2. For TE671 cells, the DMEM also contained 5% horse serum (Sigma-Aldrich). At 60–80% confluence, cells were washed with phosphate-buffered saline (PBS), harvested by trypsin/ethylenediaminetetraacetic acid (EDTA; Cambrex BioScience, Verviers, Belgium) treatment.

Electrophysiology

HEK293 cells expressing hSK1, hSK2, hSK3 or hIK were transferred to Petri dishes containing coverslips ($\varnothing$ 3.5 mm, custom made at VWR International APS, Albertslund, Denmark). Membrane currents were recorded using the whole-cell or inside-out configuration of the patch clamp technique. Patch pipettes (1.8–2.3 MΩ) were pulled from borosilicate tubes with an outside diameter of 1.32 mm (Modulohm; Copenhagen, Denmark) using a horizontal electrode puller (Zeitz Instruments; Augsburg, Germany). An electronically controlled micromanipulator (Eppendorf, Radiometer, Copenhagen, Denmark) was used for the positioning of pipettes. Cells seeded on coverslips were transferred to a 15 μl recording chamber continuously superfused at 1 ml min^{-1} at room temperature. An Ag/AgCl

pellet was fixed in the chamber. Experiments were performed using an EPC-9 amplifier (HEKA; Lambrecht, Germany) connected to a Macintosh computer by an ITC-16 interface. Data were filtered at 3 kHz. Ca^{2+}-activated K^+ currents were recorded upon application of 200 ms linear voltage ramps (from −80 to +80 mV) every 5 s from a holding potential of 0 mV. For analyses, currents were measured at −75 mV. In whole-cell experiments, the cell capacitance and series resistance (R_s below 8 MΩ, 80% compensation) were updated before each application of the voltage ramp.

For voltage-clamp experiments, an extracellular solution containing a high $[K^+]$ was used (in mM): 150 KCl, 2 $CaCl_2$, 1 $MgCl_2$ and 10 HEPES with pH adjusted to 7.4 with KOH. For current-clamp experiments, the extracellular solution contained (in mM): 140 NaCl, 4 KCl, 2 $CaCl_2$, 1 $MgCl_2$ and 10 HEPES; pH adjusted to 7.4 with NaOH.

The intracellular solutions contained 154 mM KCl and 10 mM HEPES as well as 10 mM EGTA or a combination of EGTA and NTA (10 mM in total). Concentrations of $CaCl_2$ and $MgCl_2$ needed to obtain the desired free concentrations of Ca^{2+} (0.01–10 μM, Mg^{2+} always 1 mM) were calculated by EqCal software (Cambridge, UK) and added. The free Ca^{2+} concentrations were controlled by a Ca^{2+}-sensitive electrode (WPI; Sarasota, FL, USA). All intracellular solutions were adjusted to pH 7.2 with concentrated HCl or KOH.

Fluorescence-based Tl^+ assay

HEK293 cells expressing hSK1, hSK2, hSK3 or hIK channels were seeded in 384-well, clear-bottomed, black-walled plates (Corning Inc., NY, USA). The plates were coated with poly-D-lysine (10 μg ml^{-1}), and the cells were seeded at a density of ~3×10^6 cells ml^{-1} in 20 μl DMEM containing 10% FCS per well and left overnight at 37°C in a 5% CO_2 incubator.

Before the experiment, the cells were loaded with the fluorescent dye benzothiazole coumarin acetoxymethyl ester (BTC-AM), essentially as described by Weaver *et al*. (2004). In brief, the cells were washed thrice in Cl^--free assay buffer (in mM: 140 Na^+-gluconate, 2.5 K^+-gluconate, 6 Ca^{2+}-gluconate, 1 Mg^{2+} gluconate, 5 glucose, 10 HEPES, pH 7.3), the buffer was aspirated, and 25 μl Cl^--free loading buffer (assay buffer containing an additional 2 μM BTC-AM, 2 mM amaranth and 1 mM tartrazine) was added to each well. The cells were incubated at room temperature for 1 h and, subsequently, transferred to a fluorometric imaging plate reader (FLIPR; Molecular Devices, Sunnyvale, CA, USA). For excitation, the 488 nm line of an argon laser was used, whereas on the emission side, a 540 ± 30 nm bandpass filter was inserted. Dimethylsulphoxide (DMSO) stock solutions of the compounds were diluted in Cl^--free assay buffer containing Tl_2SO_4, giving a final $[Tl^+]$ of 2 mM and final compound concentrations of 47 nM to 100 μM (final DMSO concentration <0.1%). An initial baseline signal was collected before compound addition. The cells were stimulated in quadruplicate, that is, four individual wells were stimulated per concentration. In addition, on each plate, 16 wells served as negative controls (buffer addition) and another 16 wells as positive controls (1 μM ionomycin). The data from the individual wells were background corrected by subtraction of the averaged value of the negative control wells. The data were subsequently analysed by fitting the fluorescence peak values for each concentration to the Hill equation (see below).

Calculations and statistics

EC_{50} values ($EC_{50}(Ca^{2+})$, EC_{50}(NS309) and EC_{50}(CyPPA)) were estimated from equilibrium concentration–response experiments by fitting data from individual experiments to the Hill equation (Equation 1):

$$B(C) = \frac{R^{max} * C^n}{EC_{50}^n + C^n} \quad (1)$$

where B is the current or peak fluorescence response, R^{max} is the maximal current or maximal peak fluorescent response, C is the test concentration and n is the Hill coefficient.

All results are given as the mean ± standard error of the mean (s.e.m.). Tests for statistical differences were performed by two-way analysis of variance (ANOVA) (and Bonferroni *post hoc* comparisons between individual groups) or Student's *t*-test.

Chemicals

CyPPA (see International Patent Publication WO 2006/100212) was either purchased from Specs (Delft, Netherlands) or synthesized according to the following procedure. 2,4-Dichloro-6-methylpyrimidine (7.0 g, 42.9 mmol) was dissolved in acetonitrile (20 ml). Cyclohexylamine (5.1 g, 51.5 mmol) and triethylamine (6.83 ml, 67.3 mmol) were added. The mixture was shaken in a sealed vial on a sand bath at 60°C for 12 h. Evaporation of the solvent followed by column chromatography on silica gel (60–120 mesh) with ethyl acetate/hexane as eluent, gave (2-chloro-6-methyl-pyrimidine-4-yl)-cyclohexylamine (6 g, 62%) and (4-chloro-6-methyl-pyrimidine-2-yl)-cyclohexylamine (2 g, 21%). (2-Chloro-6-methyl-pyrimidine-4-yl)-cyclohexylamine (6 g, 26.6 mmol) was dissolved in acetonitrile (20 ml) and 3,5-dimethylpyrazole (3.8 mg, 39.9 mmol) was added. The mixture was heated in a microwave oven at 130°C for 30 min. The mixture was concentrated and the residue basified with sodium hydrogen carbonate, extracted with chloroform, dried over anhydrous sodium sulphate, filtrated and evaporated. The crude product was purified by column chromatography (as described above) to give cyclohexyl-[2-(3,5-dimethyl-pyrazol-1-yl)-6-methyl-pyrimidin-4-yl]-amine (2.9 g, 38%). The melting point was 133.2–136.9°C. ^{1}H-NMR analysis in $CDCl_3$ gave the following chemical shifts: δ 6.03 (1H, s), 5.97 (1H, s), 5.14 (s, 1H), 3.53–3.65 (1H, m), 2.63 (3H, s), 2.40 (3H, s), 2.32 (3H, s), 2.00–2.03 (2H, m), 1.76–1.80 (3H, m) and 1.23–1.40 (5H, m). Analysis by mass spectrometry (LC-ESI-HRMS) of $[MH]^+$ was found to be 286.2037 Da. The calculated value was 286.20317. Elementary analysis (Department of Chemistry, University of Copenhagen, Copenhagen, Denmark): Found: C, 67.35; H, 8.21; N, 24.45; calculated for C16H23N5: C, 67.34; H, 8.12; N, 24.54.

NS309 (Strøbæk *et al*., 2004) was also synthesized at NeuroSearch A/S (Ballerup, Denmark). Clotrimazole (Clot) and charybdotoxin (ChTX) were purchased from Sigma-

Aldrich and bicuculline methobromide (BMB) from MP Biomedicals Inc. (Illkirch, France). All other chemicals were purchased from regular commercial sources and were of the purest grade available. Clotrimazole, BMB, NS309 and CyPPA were dissolved in DMSO and diluted at least 1000 times in the experimental solutions.

Results

Effects of CyPPA on recombinant hSK3 and hIK channels in the whole-cell configuration

Figure 1a shows the chemical structures of CyPPA as well as of the reference compound NS309. CyPPA is a small (MW: 285), trisubstituted pyrimidine that belongs to a completely different compound class from that of the prototype IK/SK channel activators 1-EBIO and NS309, which are rigid, fused heteroaromatic compounds. In Figure 1b and c, the effect of CyPPA is compared to that of NS309. Whole-cell patch clamp recordings were performed in symmetrical high K^+ solutions using HEK293 cells stably expressing hSK3 and hIK, respectively. For both figures, the panels to the left show the currents recorded upon application of voltage ramps and the panels to the right show the time courses of the experiments (analysed as the current at −75 mV). Application of 40 nM NS309 activated both hSK3 (Figure 1b) and hIK (Figure 1c) channels, with the largest effect on hIK channels (8.5±0.4 ($n=3$)-fold increase in current compared to 1.9±0.1 ($n=5$)-fold increase in current for hSK3 channels; $P<0.0001$). In contrast to this, CyPPA prominently activated the hSK3 current when applied at 300 nM (3.0±0.4-fold increase, $n=5$), whereas it was inactive at hIK even at a concentration of 10 μM (1.1±0.2-fold increase, $n=3$). The figures also illustrate that the hSK3 and hIK channels are inhibited by their respective blockers to the same extent in the absence and presence of CyPPA. BMB applied at 30 μM blocked hSK3 channels 70±3.4 and 78±4.1% ($n=5$) in the absence or presence of CyPPA, whereas ChTX applied at 30 nM blocked hIK channels 50±3.7 and 46±5% ($n=3$), respectively, in the absence or presence of CyPPA, in good agreement with previous reports on SK and IK channel block by these compounds (Jensen *et al*., 1998; Strøbæk *et al*., 2000).

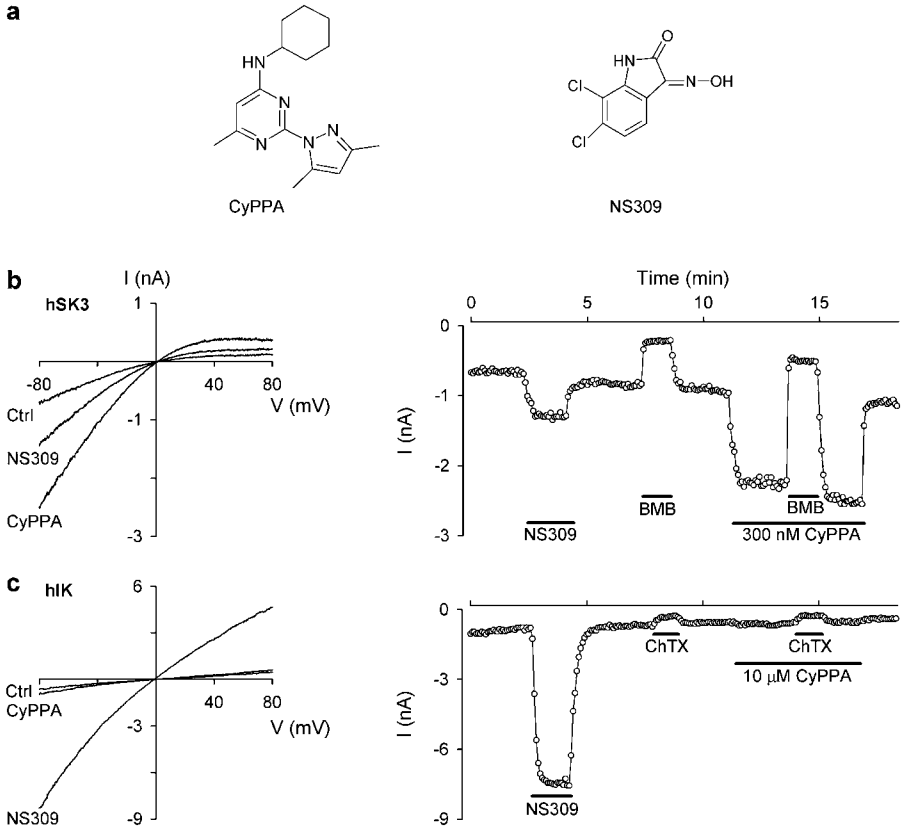

Figure 1 CyPPA is a positive modulator of hSK3 but not hIK channels. (**a**) Chemical structures of the subtype-selective SK channel activator CyPPA and the pan-selective compound NS309. (**b**) The left panel shows whole-cell current–voltage (*I-V*) relationships from a HEK293 cell expressing hSK3. The currents were recorded upon application of 200 ms long voltage ramps (−80 to +80 mV) elicited every 5 s from a holding potential of 0 mV. The free $[Ca^{2+}]$ in the pipette solution was buffered at 0.3 μM and the $[K^+]$ was 154 mM in the intra- as well as extracellular solutions. The traces were obtained before (Ctrl) and during application of 40 nM NS309 or 300 nM CyPPA as indicated. The right panel shows the current at −75 mV as a function of time. The first 7 min after obtaining the whole-cell configuration are not shown. During this period the hSK3 current increased as a result of Ca^{2+} equilibration between the pipette solution and the cell; also 0.1% DMSO was shown to be without effect on the currents. NS309 (40 nM), BMB (30 μM) and CyPPA (300 nM) were present in the bath solution as indicated by the bars. BMB inhibited the current by 75 and 77% in the absence and presence of CyPPA, respectively. (**c**) Same experimental conditions as in (**b**) but using a hIK-expressing HEK293 cell. The hIK current was activated by 40 nM NS309 and inhibited by 30 nM ChTX. The hIK current was inhibited by 54 and 51% before and during application of 10 μM CyPPA.

CyPPA affinities for the individual SK channel subtypes studied by inside-out patches

Inside-out patches enable measurements under controlled intracellular [Ca^{2+}] and furthermore it is feasible to obtain full activation curves for Ca^{2+} and test compounds. Multi-channel inside-out patches were pulled from hSK3, hSK2 and hSK1 expressing HEK293 cells. Figure 2a shows typical SK3 current traces measured upon application of voltage ramps in symmetrical K^+ concentrations with $[Ca^{2+}]_i$ buffered at 0.2 μM and 10 μM (solid lines) yielding 2.5 and 100% activation, respectively (data from full Ca^{2+}-activation curves, see Figure 3). At 0.2 μM Ca^{2+}, application of increasing concentrations of CyPPA (0.1–100 μM, dotted curves) to the inside of the patch, caused a concentration-dependent increase of the hSK3 current, reaching nearly 100% activation (compared to 10 μM Ca^{2+}) at the highest concentration. Note that the characteristic inward rectification of the current was maintained when activated by a combination of low Ca^{2+} and CyPPA. Figure 2b shows the time course of this experiment. A number of identical experiments were performed and the data were normalized to the maximal current attained at 10 μM Ca^{2+} in the individual experiments. Figure 2c shows the CyPPA concentration–response plot for hSK3, hSK2 and hSK1 based on these averaged and normalized data ($n=3$–5). Fitting the data to Equation 1 resulted in an EC_{50} value of 5.6 ± 1.6 μM for activation of hSK3. The corresponding Hill coefficient was 1.7 ± 0.2 and the efficacy relative to 10 μM Ca^{2+} was 90 ± 1.8%. CyPPA activated hSK2 with an EC_{50} value of 14 ± 4 μM, a Hill coefficient of 2.0 ± 0.1 and an efficacy of 71 ± 1.8% (middle curve), whereas no activation was observed with hSK1 at concentrations of CyPPA up to 100 μM (lower curve). CyPPA was not tested on hIK in inside-out experiments due to a prominent rundown of channel activity in excised patches. For comparisons, the non selective SK channel activators, NS309, DC-EBIO and 1-EBIO activated hSK3 with EC_{50} values of 0.3 ± 0.03 μM ($n=3$), 16 ± 2 μM ($n=3$) and 1040 ± 150 μM ($n=5$), respectively (not shown).

Similar effects of CyPPA were obtained in experiments with the corresponding rat SK3 and SK2 channels (results not shown). As the rat isoform of the recombinant SK1 channel does not express as a homomer, we have not been able to investigate selectivity towards the rat SK1 channel.

The effect of CyPPA on the Ca^{2+}-activation curves for SK channels elucidated using inside-out patches

Figure 3a (left panel) shows the time course of an experiment where the effect of 10 μM CyPPA was tested at 0.01, 0.2 and 10 μM intracellular Ca^{2+}. No effect of CyPPA was observed at a very low (0.01 μM Ca^{2+}) or a very high (10 μM Ca^{2+}) degree of hSK3 channel activation, whereas a prominent stimulation (from 6 to 80% of full activation) occurred at the intermediate Ca^{2+} concentration. Figure 3a (right panel) shows the Ca^{2+}-activation curves for hSK3 in the absence and presence of 10 μM CyPPA. The Ca^{2+} activation curve was significantly affected by CyPPA ($P<0.001$, two-way ANOVA) and the main effect is clearly to left-shift the activation curve for Ca^{2+}, but we also consistently found a reduced Hill coefficient (from 6.3 ± 0.4 to 3.6 ± 0.2). The influence of CyPPA on the Ca^{2+} activation curve for hSK2 and hSK1 was investigated under identical experimental conditions (Figure 3b and c). CyPPA also significantly ($P<0.001$, two-way ANOVA) affected the Ca^{2+} activation curve at hSK2 channels, although less prominently than at hSK3. In contrast to the effect on hSK3, however, CyPPA induced a small reduction of the current at high Ca^{2+} concentrations (Figure 3b, left panel). Consequently, the effect of CyPPA on

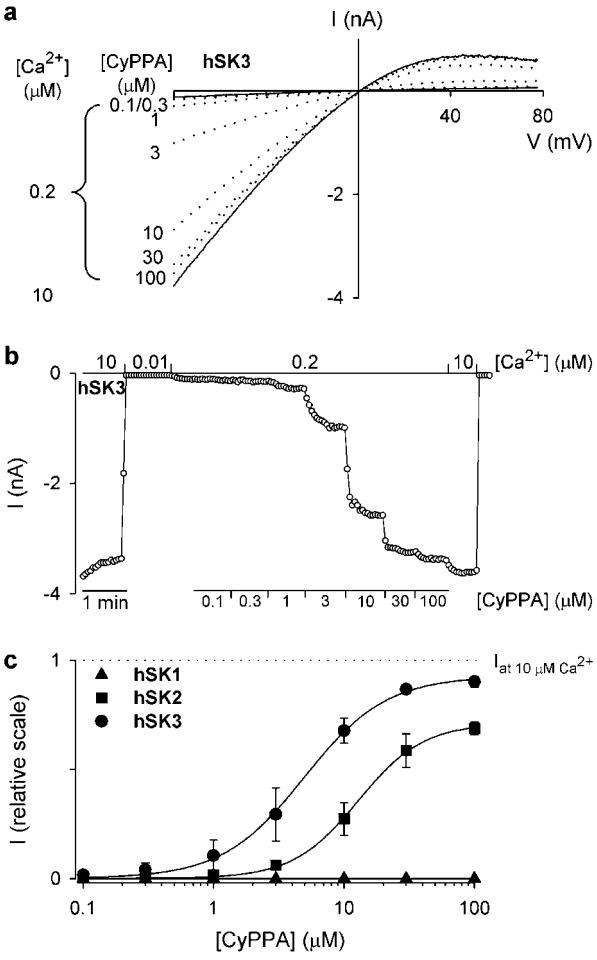

Figure 2 CyPPA is a SK subtype-selective potentiator. (**a**) *I-V* relationships measured on an inside-out patch obtained from a HEK293 cell stably expressing hSK3. The voltage protocol was as described in the legend to Figure 1. The solid lines are *I-V* relationships measured at a bath/intracellular [Ca^{2+}] of 0.2 or 10 μM in the absence of CyPPA. The dotted lines are *I-V* relationships obtained in the presence of CyPPA (0.2 μM Ca^{2+}, [CyPPA] from 0.1 to 100 μM as indicated). (**b**) hSK3 current at −75 mV as a function of time. The patch was exposed to a bath/intracellular [Ca^{2+}] of 0.01, 0.2 or 10 μM as indicated. In the presence of 0.2 μM Ca^{2+}, the patch was exposed to increasing CyPPA concentrations (0.1–100 μM). (**c**) Concentration–response relationship for CyPPA obtained from experiments conducted as in (**b**). Currents were normalized with respect to the effect of 10 μM Ca^{2+}, which induces maximal SK channel activity, and data points represent mean$\pm$s.e.m. of 3–5 experiments. The solid lines are the fit of the Hill equation to mean data. EC_{50} values and Hill coefficients, estimated from separate experiments were as follows: hSK3, 5.6 ± 1.6 μM and 1.7 ± 0.2 ($n=3$); hSK2, 14 ± 4 μM and 2.0 ± 0.1 ($n=3$); hSK1, not detectable. Efficacies with respect to 10 μM Ca^{2+} were as follows: hSK3, 90 ± 1.8%; and hSK2, 71 ± 1.8%.

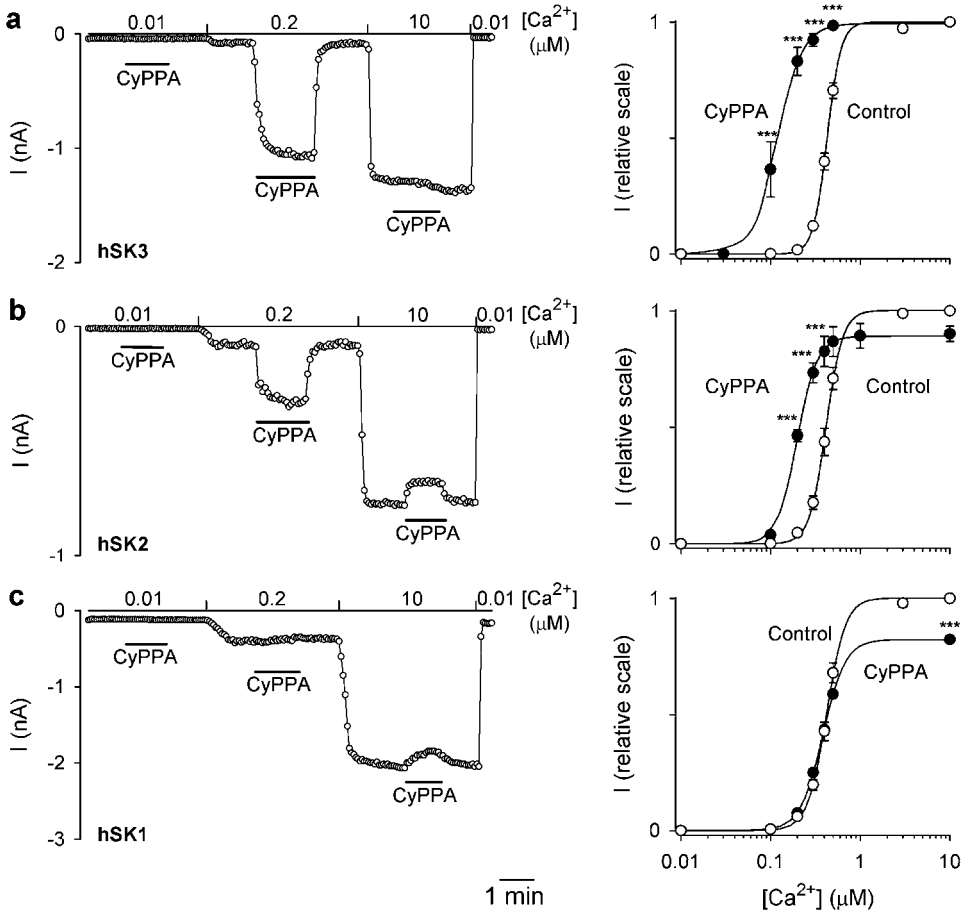

Figure 3 SK subtype-dependent effects of CyPPA on the Ca^{2+} activation curves. In the left panels, currents at −75 mV are depicted as a function of time. Currents were measured from inside-out patches obtained from HEK293 cells stably expressing hSK3 (**a**), hSK2 (**b**) or hSK1 (**c**). The patches were exposed to a bath/intracellular [Ca^{2+}] of 0.01, 0.2 or 10 μM as indicated, and CyPPA (10 μM) was applied at the different [Ca^{2+}] as shown by the bars. In the right panels, the Ca^{2+} concentration–response relationships for hSK3, hSK2 and hSK1 are depicted in the absence or presence of 10 μM CyPPA. Currents from individual patches were normalized with respect to the effect of 10 μM Ca^{2+} (in the absence of CyPPA). The solid lines are the fit of the Hill equation to mean data. The following $EC_{50}(Ca^{2+})$ and Hill coefficients were estimated from separate experiments: hSK3, 0.43±0.01 μM and 6.3±0.4 (control, $n=14$), 0.12±0.02 μM and 3.4±0.2 (+10 μM CyPPA, $n=3$); hSK2, 0.42±0.02 μM and 5.2±0.1 (control, $n=8$), 0.20±0.01 and 3.9±0.3 (+10 μM CyPPA, efficacy: 91±4%, $n=3$); hSK1, 0.42±0.01 μM and 4.5±0.2 (control, $n=8$), 0.38±0.03 μM and 3.5±0.2 (+10 μM CyPPA, efficacy: 84±7%, $n=3$); ***$P<0.001$ compared to corresponding control values (Bonferroni *post hoc* comparisons).

the Ca^{2+} activation curve for hSK2 is more complex than for hSK3, consisting of a leftward shift and a slight reduction in the maximal activation (right panel). No overall influence on the activation of hSK1 was observed at any Ca^{2+} concentration (Figure 3c, left panel, $P>0.05$, two-way ANOVA), but the slight reduction in current at high Ca^{2+} concentrations, as was observed for hSK2, was also seen with hSK1 (right panel).

The mechanism of action of CyPPA was compared to that of the IK/SK channel activator, NS309, by performing detailed concentration–response evaluations on the hSK3 activation curves for Ca^{2+}. Figure 4a shows the results for NS309 (0.03–30 μM) and Figure 4b shows the corresponding results obtained with CyPPA (0.1–100 μM). The effects of the two compounds are qualitatively very similar: both produce a concentration-dependent leftward shift of the activation curve for Ca^{2+}, without increasing the maximal degree of SK3 channel activation. This is quantified for both compounds in Figure 4c, by plotting the EC_{50} values for Ca^{2+} ($EC_{50}(Ca^{2+})$) vs the concentration of NS309 and CyPPA, respectively. Both plots reveal saturating curves with a 350–400 nM maximal change in the Ca^{2+}-sensitivity of the drug-modified hSK3 channel, reducing the $EC_{50}(Ca^{2+})$ to below 75 nM. This suggests that, in the presence of high concentrations of any of these positive modulators, the SK3 channel can be activated at the resting intracellular Ca^{2+} concentration. The EC_{50} values for the leftward shift in the hSK3 activation curve for Ca^{2+} were 0.15 μM for NS309 and 1.01 μM for CyPPA.

Interaction studies with CyPPA and NS309 at the hSK1 channel

Given the very similar functional effects of CyPPA and NS309 on hSK3, these compounds might be anticipated to interact with this channel in a similar fashion, perhaps even interacting with the same binding site. The question is then: how does selectivity against hSK1 arise? The straightforward possibility is that CyPPA does not bind at all to hSK1. An

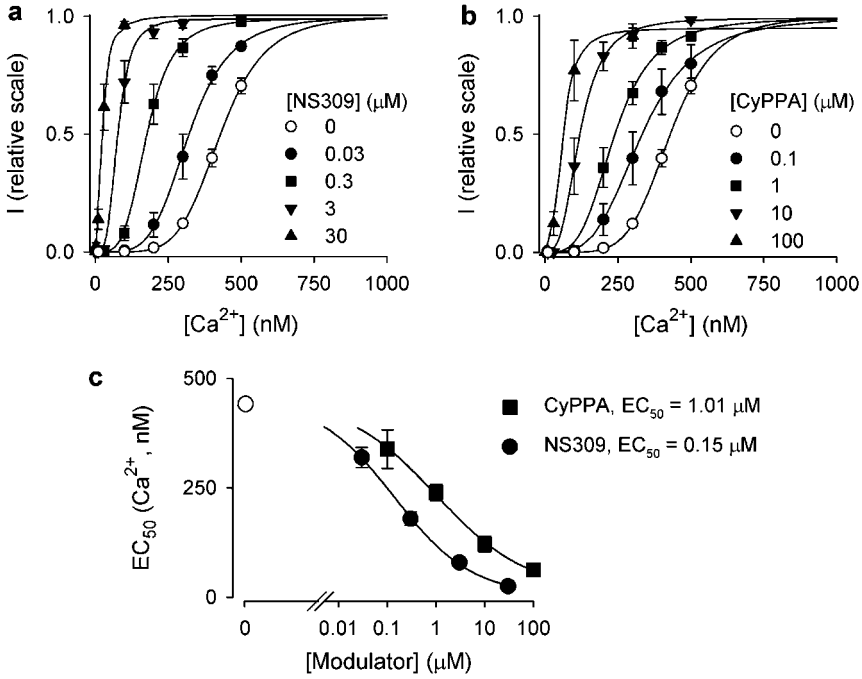

Figure 4 NS309 and CyPPA modulate the Ca^{2+} sensitivity of SK3 channels in a similarly concentration-dependent manner. Ca^{2+} concentration–response relationships for hSK3, depicted in the absence or presence of increasing concentrations of NS309 (**a**) or CyPPA (**b**) ($n = 3$–14). Currents from individual patches were normalized with respect to the effect of 10 μM Ca^{2+} (in the absence of compound). The solid lines are the fit of data to the Hill equation, yielding the following $EC_{50}(Ca^{2+})$ and Hill coefficients: (**a**) control: 429 nM and 5.6; 0.03 μM NS309: 322 nM and 4.6; 0.3 μM NS309: 177 nM and 4.0; 3 μM NS309: 77 nM and 3.6; 30 μM NS309: 24 nM and 2.1; (**b**) Control: 429 nM and 5.6; 0.1 μM CyPPA: 332 nM and 3.7; 1 μM CyPPA: 239 nM and 3.6; 10 μM CyPPA: 119 nM and 3.1; 100 μM CyPPA: 59 nM and 2.8. At 100 μM CyPPA, the fitted maximal value was 95%, for all other experiments the fitted maximal value was >99% with respect to the effect of 10 μM Ca^{2+}. (**c**) $EC_{50}(Ca^{2+})$ as a function of the NS309 or CyPPA concentration. $EC_{50}(Ca^{2+})$ values were obtained from the experiments summarized in (**a**) + (**b**). The solid lines are the fit of the Hill equation to mean data yielding the following minimal values for $EC_{50}(Ca^{2+})$, EC_{50} and Hill coefficients: NS309: 24 nM, 0.15 μM and 0.6; CyPPA: 59 nM, 1.01 μM and 0.5.

alternative possibility is that CyPPA binds, but that it selectively lacks the capability of transmitting the stimulatory action to the gating machinery of hSK1. To see if CyPPA possibly interacts with or even occludes the activating effect of NS309 an interaction study with these two compounds on hSK1 was performed. Figure 5a shows the time course of an inside-out experiment addressing this question: After maximal activation/deactivation of the hSK1 channel by high and low Ca^{2+}, respectively, the activity was adjusted to a low level by 0.2 μM intracellular Ca^{2+}. As expected, addition of 10 μM NS309 fully activated the hSK1 channel. After washout of NS309, 10 μM CyPPA was added for 1.5 min (no activation) before 10 μM NS309 was co-applied with CyPPA for another 1.5 min. Clearly, NS309 activated/deactivated the hSK1 channel as fully and as fast as in the absence of CyPPA. In the bar diagrams of Figure 5b, the increase in hSK1 current induced by 0.1 and 10 μM NS309 in the presence and absence of 10 μM CyPPA is shown. Clearly, the presence of CyPPA is not a significant hindrance for the NS309-induced activation of hSK1 even at low concentrations of NS309.

Effect of CyPPA on intact, unclamped cells in population using a fluorescent Tl^+ flux assay

As with all K^+-selective ion channels (for data on KcsA, see LeMasurier *et al*., 2001), SK channels are permeable for Tl^+ and we exploited this feature to carry out an influx assay

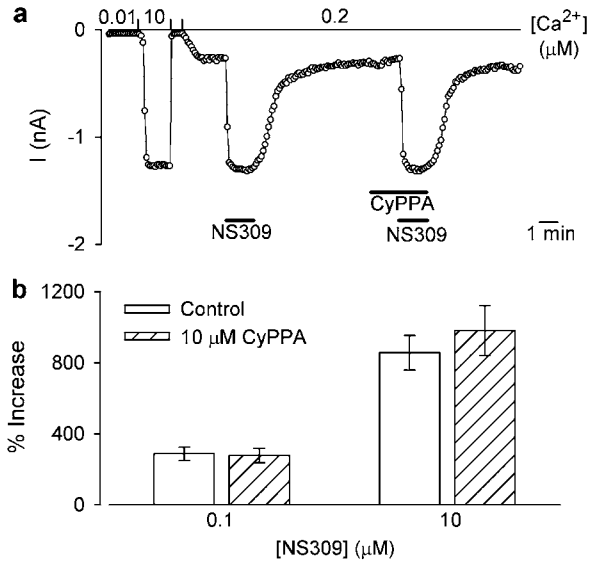

Figure 5 CyPPA does not inhibit NS309-induced activation of hSK1. (**a**) hSK1 current at −75 mV as a function of time. The current was measured from an inside-out patch obtained from a HEK293 cell stably expressing hSK1. The patch was exposed to a bath/intracellular $[Ca^{2+}]$ of 0.01, 0.2 or 10 μM as indicated. NS309 (10 μM) was added at a $[Ca^{2+}]$ of 0.2 μM either in the absence or presence of 10 μM CyPPA. (**b**) Increase in hSK1 current induced by NS309 (0.1 or 10 μM) in the absence or presence of 10 μM CyPPA; $n = 6$–13.

with cells loaded with a Tl^+-sensitive fluorescent dye (BTC-AM). Figure 6a shows the Ca^{2+}-induced activation of hSK1-3 and hIK expressed in HEK293 cells as measured by the fluorescence increase over time. The effect of 1 μM ionomycin (maximal response) was compared to the responses obtained with 10 and 100 μM CyPPA, respectively. In the hSK3 and hSK2 cell lines, CyPPA gave a clear increase in fluorescence, whereas no response was detected using the hSK1 and hIK cell lines. The distinct Tl^+ fluorescence increase seen upon CyPPA application to hSK3 and hSK2 cell lines emphasizes that CyPPA is capable of activating SK channels at the resting concentration of intracellular Ca^{2+} prevailing in these cells. In SK-expressing cells both the ionomycin- and CyPPA-induced signals were completely blocked by apamin, whereas the ionomycin-induced fluorescence from the hIK cell line was blocked by clotrimazole (data not shown). In contrast to CyPPA, NS309 concentration dependently increased the fluorescence from all four cell lines (data not shown). Figure 6b shows the compiled concentration–response curves (normalized to the maximal ionomycin response) from the experiments with CyPPA. The following selectivity sequence was found from the Tl^+ experiments: SK3 ($EC_{50} = 4.3 \pm 1.0$ μM; efficacy $= 105 \pm 2\%$); SK2 ($EC_{50} = 13 \pm 2.0$ μM; efficacy $= 91 \pm 4\%$); SK1 (undetectable); hIK (undetectable).

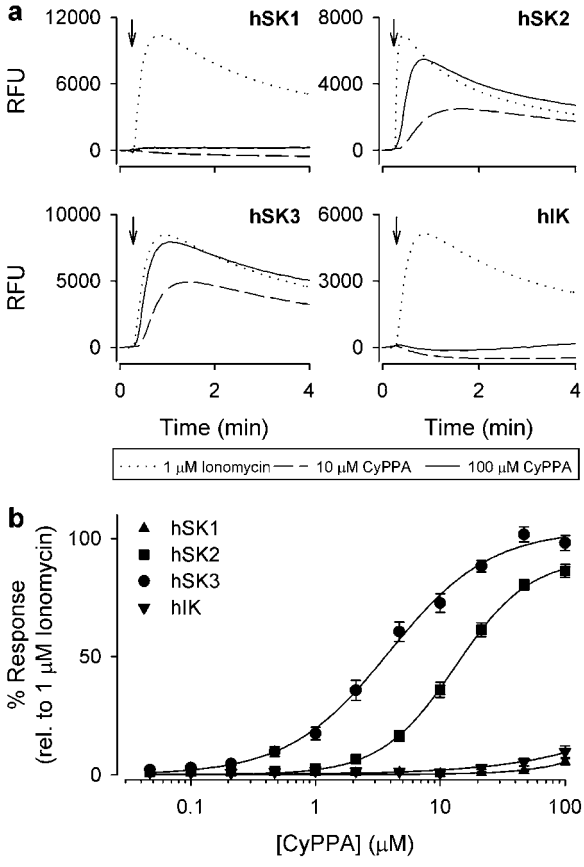

Figure 6 Subtype selectivity of CyPPA in a Tl^+-based FLIPR assay. (**a**) Relative fluorescence units (RFUs) measured over time in HEK293 cells expressing hSK1, hSK2, hSK3 or hIK channels loaded with the fluorescent dye BTC-AM (see Materials and methods). At the time indicated by the arrow, ionomycin (1 μM) or CyPPA (10 or 100 μM) dissolved in Tl^+-containing Cl^--free assay buffer was added to the wells. Opening of either channel subtype permits an influx of Tl^+, resulting in an increase in RFUs due to interaction of Tl^+ with BTC. (**b**) Concentration–response relationship for CyPPA on the four cell types expressing hSK1, hSK2, hSK3 or hIK, based on experiments similar to those shown in (**a**). The increase in RFUs was normalized to the effect of 1 μM ionomycin. The data points represent the mean $\pm$ s.e.m. of four independent experiments. The solid lines are the fit of mean data to the Hill equation. The following efficacies, EC_{50} values and Hill coefficients were estimated from separate experiments ($n = 4$): hSK3, $105 \pm 2\%$, 4.3 ± 1.0 μM and 1.1 ± 0.1; hSK2, $91 \pm 4\%$, 13.0 ± 2.0 μM and 1.6 ± 0.2; hSK1, n.d. hIK, n.d.

Effects of CyPPA on endogeneously expressed SK3 and IK channels in the whole-cell configuration

The selectivity pattern for CyPPA described here is based on the effect on recombinant channels overexpressed in a mammalian cell line. To verify that the same selectivity properties of CyPPA apply to endogenous SK/IK channels, we also tested it on the SK3 expressing TE671 cells as well on the IK expressing HeLa cells. Figure 7a shows whole-cell current-voltage ramps (symmetrical K^+) from a TE671 cell. Application of 10 μM CyPPA stimulated the current by a factor of 2, which was essentially the same effect as obtained with a subsequent 1 μM NS309 application. The experiment was ended by application of 100 μM of the selective SK channel blocker BMB. A very similar experimental protocol was applied to the HeLa cells (Figure 7b; note the much less pronounced inward rectification compared to the SK3-mediated current from TE671 cells, compare also with Figure 1). CyPPA at 10 μM had no effect on the IK current, whereas NS309 at 1 μM exerted a significant activation. Again the experiment was concluded with the application of the established IK blocker, clotrimazole, at a concentration of 1 μM. Figure 7c and d show corresponding experiments with TE671 and HeLa cells recorded under current-clamp conditions with cells superfused with near-physiological saline. Both cells exhibited a rather depolarized resting membrane potential when equilibrated with a pipette solution buffered at 100 nM Ca^{2+}. In accordance with the voltage-clamp experiments, CyPPA (10 μM) strongly hyperpolarized the TE671 cell, whereas no effect was observed on the IK channel expressing HeLa cell. Both cell lines responded with substantial hyperpolarization upon application of NS309.

Finally, to investigate selectivity towards other classes of ion channels, CyPPA was tested on a number of cloned ion channels expressed in HEK293 cells (hERG, BK, $K_V7.2 + 7.3$, $Na_V1.2$) as well as voltage-dependent Na^+ channels, delayed rectifier K^+ channels, and high threshold voltage-dependent Ca^{2+} channels from rat dorsal root ganglia neurons (see Table 1). The compound did not activate any ion channel tested except for SK3 and SK2, indicating that this effect is specific for SK channels. However, CyPPA caused an inhibition of BK (half-maximal inhibitory concentration (IC_{50}) $= 5.5$ μM) and of Na_V ($IC_{50} \approx 10$ μM) channels.

Discussion and conclusions

In this study we have identified and characterized CyPPA, a subtype-selective positive modulator of small conductance

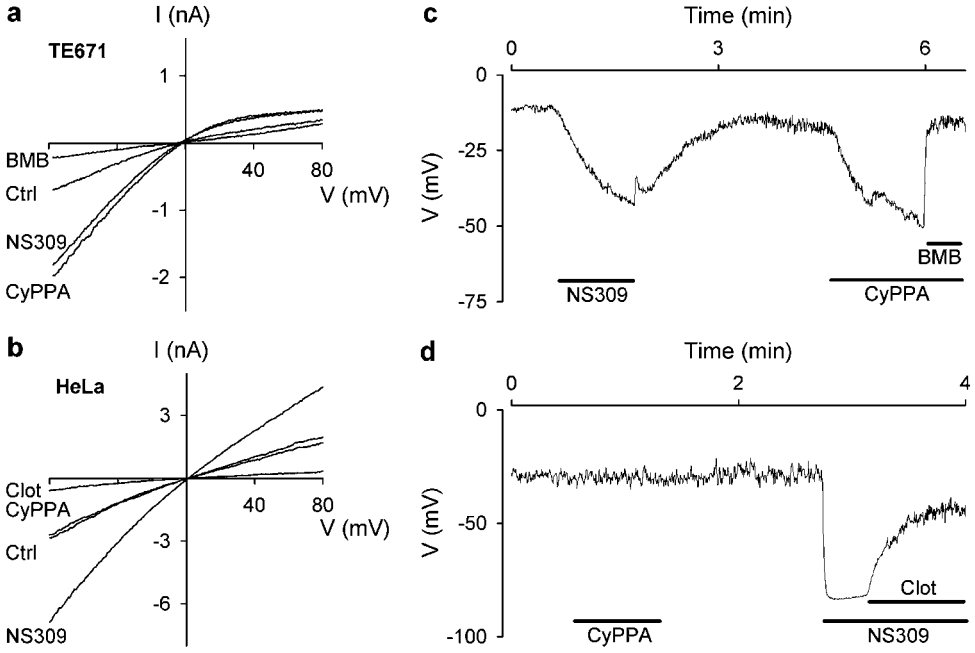

Figure 7 CyPPA activates the endogenous SK channels in TE671 cells but not the endogenous IK channels in HeLa cells. Whole cell *I-V* relationships measured in a TE671 (**a**) or HeLa (**b**) cell upon application of 200 ms long voltage ramps (−80 to + 80 mV) elicited every 5 s from a holding potential of 0 mV; $[Ca^{2+}]$ in the pipette solution was 0.4 μM. Whole-cell *I-V* relationships were measured in the absence of compound (Ctrl) and in the presence of NS309 (1 μM), or CyPPA (10 μM). BMB (100 μM) was applied as an inhibitor of SK channel activity in TE671 cells (**a**) and clotrimazole (clot, 1 μM) as an inhibitor of IK channels in HeLa cells (**b**). Membrane potential measured under current-clamp conditions in a TE671 cells (**c**) or a HeLa cell (**d**). The cells were exposed to a near-physiological K^+ gradient at an intracellular $[Ca^{2+}]$ of 0.1 μM. NS309 (1 μM) and CyPPA (10 μM) were applied to the extracellular solution as indicated and experiments terminated by addition of BMB (100 μM, C) or clot (1 μM, D); $n = 3$–5.

Table 1 Effect of CyPPA on selected ion channels

Ion channel	*Cell type*	*Result (μM)*
$K_{Ca}1.1$ (BK)	HEK293	$IC_{50} = 5.5 \pm 1.3$ ($n = 6$)
$K_v7.2 + 7.3$ (KCNQ2 + 3)	HEK293	No effect at 30 ($n = 3$)
$K_v11.3$ (hERG)	HEK293	No effect at 10 ($n = 4$)
$Na_v1.2$	HEK293	$IC_{50} = 10 \pm 1.9$ ($n = 3$)
Voltage-dependent K^+	DRG	$IC_{50} = 68 \pm 8.8$ ($n = 5$)
Voltage-dependent Na^+	DRG	$IC_{50} = 11 \pm 0.48$ ($n = 3$)
Voltage-dependent Ca^{2+}	DRG	No effect at 10 ($n = 3$)

Abbreviations: BK, large conductance Ca^{2+}-activated K^+ channel; CyPPA, cyclohexyl-[2-(3,5-dimethyl-pyrazol-1-yl)-6-methyl-pyrimidin-4-yl]-amine; DRG, dorsal root ganglion; HEK, human embryonic kidney; hERG, human ether-a-go-go-related gene; IC_{50}, half-maximal inhibitory concentration.
CyPPA was tested in whole-cell voltage-clamp experiments using standard experimental protocols using recombinant ion channels stably expressed in HEK293 cells or endogeneously expressed channels in isolated DRG neurons. IC_{50} values were calculated from the blocker kinetics, assuming that $IC_{50} = K_d = (k_{off})\ (k_{on})^{-1}$, as described in Strøbæk *et al.* (2006).

Ca^{2+}-activated K^+ channels. Using the whole-cell as well as the inside-out patch-clamp technique, CyPPA was shown to stimulate recombinant hSK3 and hSK2 channel activity, whereas it was inactive on hSK1 and hIK channels. Using the same cell lines, the selectivity sequence was confirmed with a fluorescence-based Tl^+ flux assay with unclamped populations of intact cells. The described selectivity of CyPPA holds true for endogeneously expressed channels as well: CyPPA activated SK channels in the TE671 human medulloblastoma cell line (predominantly SK3, Carignani *et al.*, 2002) both in voltage-clamp studies with symmetric K^+ distributions, and in current-clamp studies using near-physiological ion gradients. In contrast, using identical experimental conditions, the compound had no activity on IK channels from HeLa cells (Sauvé *et al.*, 1986). Hence, the selectivity profile of CyPPA is not a cloning artifact, is not related to the level of expression or the expression system used, and is not linked to a specific experimental technique.

Using inside-out patches, the Ca^{2+} concentration giving 50% channel activation, the $EC_{50}(Ca^{2+})$ value, was found to be 420–430 nM for all the human SK channel subtypes. CyPPA was shown to induce a leftward shift in the activation curves for Ca^{2+} on hSK3 and, to a lesser degree, on hSK2 channels, whereas no shift was recorded for the hSK1 channel. A detailed analysis of the concentration dependence of the CyPPA-mediated effect on $EC_{50}(Ca^{2+})$ was performed for the hSK3 channel: CyPPA left-shifts the Ca^{2+}-activation curve with an EC_{50} value of 1.01 μM to a limiting minimal $EC_{50}(Ca^{2+})$ value of 59 nM. This implies that in presence of high concentrations of CyPPA, the hSK3 channel can be activated by the resting intracellular Ca^{2+} concentration of most cells. For comparison, a similar analysis of hSK3 activation was performed for the potent prototype IK/SK activator NS309. Qualitatively the two compounds acted similarly, although NS309 was significantly more potent ($EC_{50}(NS309) = 150$ nM) and caused a slightly larger maximal shift in the $EC_{50}(Ca^{2+})$ value (to 24 nM). Their similar modes of action on hSK3 might suggest that NS309 and CyPPA bind to the same site and modulate

channel activity by a similar mechanism. There was, however, no apparent interaction between NS309 and CyPPA on the hSK1 channels. The selectivity of CyPPA could therefore result from lack of binding to a common modulator site of hSK1-3 and hIK or indicate that additional sites are present in hSK2 and hSK3 subtypes. Mutagenesis work has localized the 1-EBIO interaction site of SK2 to the C-terminal region close to the CAMBD (Pedarzani *et al*., 2001). A similar approach could be used to elucidate regions important for CyPPA action and whether NS309 and CyPPA possibly act through a common site.

The activation of neuronal SK channels by intracellular Ca^{2+} occurs by a fast association/dissociation reaction (Xia *et al*., 1998), allowing SK channel opening and generation of the mAHP following single or a few action potentials. In presence of 1-EBIO, the deactivation time constant is greatly prolonged (Pedarzani *et al*., 2001) and the use of 1-EBIO and other positive modulators of IK/SK have revealed pharmacological sensitization of SK channels as a principle for intervention with CNS hyperactivity disorders. However, owing to the lack of selectivity of these channel modulators, the specific SK subtypes responsible are often ill –defined, particularly with *in vivo* studies. 1-EBIO eliminates low Mg^{2+}-induced network oscillations in cultures of dissociated cortical neurons, suggesting a role for positive modulators of SK channels in epilepsy (Pedarzani *et al*., 2001). Accordingly, using hippocampal slices, 1-EBIO was shown to be an effective general inhibitor of *in vitro* epileptiform activity in CA3 neurons, both when induced by increasing glutamatergic drive (low extracellular Mg^{2+}), general excitability (slightly increased extracellular K^+), or via GABA-ergic disinhibition using antagonists of GABA-A (pentylenetetrazole, gabazine) and GABA-B (CGP55845)-mediated neurotransmission, respectively (Lappin *et al*., 2005). Recently, the anticonvulsive effect of 1-EBIO has been confirmed *in vivo* using the mouse maximal electroshock and the pentylenetetrazole models of epilepsy; notably, however, CNS-related adverse effects were observed at the effective doses (Anderson *et al*., 2006).

SK channels contribute to the precision of autonomous activity in several pacemaking CNS neurons. Dopaminergic neurons in the substantia nigra compacta exhibit a slow (1–3 Hz) regular electrical activity when recorded in slices of the midbrain (Shepard and Bunney, 1988). 1-EBIO reduces the frequency of this spontaneous activity (Wolfart *et al*., 2001), an effect that is blocked by apamin. Pharmacological modulation of SK channels also affects firing of dopaminergic neurons *in vivo*: the highly irregular firing mode recorded by extracellular single-unit recording is regularized by systemic administration of 1-EBIO, whereas local apamin (Ji and Shepard, 2006) or *N*-methyl-laudanosine (Waroux *et al*., 2005) application induce burst firing. These observations may help explain the action of the centrally acting muscle relaxant drugs, zoxazolamine and chlorzoxazone (Matthews *et al*., 1984). SK channels are also essential for firing control in cerebellar Purkinje neurons, where 1-EBIO and apamin exert opposite effects and induce pace-making and bursting, respectively (Cingolani *et al*., 2002). Recently, elegant experiments have been performed with a disease model of Human Ataxia Type 2 (Walter *et al*., 2006). Using an ataxic tottering mouse (which carries a similar loss-of-function mutation in P/Q type Ca^{2+} channels as human patients), the precision of cerebellar Purkinje cell pacemaker firing was shown to be significantly impaired owing to inefficient periodic activation of SK channels. By increasing the Ca^{2+} sensitivity of the SK channels via local chronic administration of 1-EBIO to the cerebellum, the precision of Purkinje cell firing was restored and partial correction of the ataxic behaviour was attained.

The identification of a subtype-selective SK channel activator, such as CyPPA, has a number of consequences. Firstly, this finding strongly indicates that positive modulation of SK channel gating involves amino-acid residues on the α-subunit that are nonconserved among the SK subtypes and also compared to the IK channel. In this respect, the selectivity profile of CyPPA is narrower than the recently described negative gating modulator, NS8593 (Strøbæk *et al*., 2006), which is inactive on IK, although it does not discriminate between the SK members. Secondly, as a pharmacological tool, CyPPA may be used in parallel with the IK/SK openers such as 1-EBIO and NS309 to distinguish SK3/SK2 from SK1-mediated pharmacological responses; this is particularly important for the SK2 and SK1 subtypes, which show considerable overlap in expression in the neocortical and hippocampal regions (Sailer *et al*., 2004). This also applies to peripheral cells where both SK and IK channels are present, for instance in vascular endothelial cells (SK3/IK, Eichler *et al*., 2003). However, it must be stressed that CyPPA, owing to its inhibitory action on Na^+ channels, should be used cautiously in complex biological systems such as epilepsy models, where the causality of responses may be misinterpreted. Thirdly, CyPPA may be used to address an important selectivity question – which this study does not consider – namely whether CyPPA can activate heteromeric SK channels (Benton *et al*., 2003; Strassmaier *et al*., 2005). The answer to this question is obviously of pharmacological relevance, in particular for SK1 and SK2, but it may also help to understand if the physical binding site for SK channel openers possibly involves one or more SK α-subunits.

Acknowledgements

Aino Munch is acknowledged for help with the thallium flux characterization. Jette Sonne, Vibeke Meyland-Smith and Anne Stryhn Meincke are acknowledged for help with the initial patch-clamp characterization of CyPPA. Dr Gordon John Blackburn-Munro is greatly acknowledged for reading this paper and correcting the language.

Conflict of interest

The authors state no conflict of interest.

References

Anderson NJ, Slough S, Watson WP (2006). *In vivo* characterisation of the small-conductance K_{Ca} (SK) channel activator 1-ethyl-2-benzimidazolinone (1-EBIO) as a potential anticonvulsant. *Eur J Pharmacol* **546**: 48–53.

Benton DC, Monaghan AS, Hosseini R, Bahia PK, Haylett DG, Moss GW (2003). Small conductance Ca^{2+}-activated K^+ channels formed by the expression of rat SK1 and SK2 genes in HEK 293 cells. *J Physiol* **553**: 13–19.

Bildl W, Strassmaier T, Thurm H, Andersen J, Eble S, Oliver D *et al*. (2004). Protein kinase CK2 is coassembled with small conductance Ca^{2+}-activated K^+ channels and regulates channel gating. *Neuron* **43**: 847–858.

Bond CT, Maylie J, Adelman JP (2005). SK channels in excitability, pacemaking and synaptic integration. *Curr Opin Neurobiol* **15**: 305–311.

Bond CT, Herson PS, Strassmaier T, Hammond R, Stackman R, Maylie J *et al*. (2004). Small conductance Ca^{2+}-activated K^+ channel knock-out mice reveal the identity of calcium-dependent afterhyperpolarization currents. *J Neurosci* **24**: 5301–5306.

Cao Y, Dreixler JC, Roizen JD, Roberts MT, Houamed KM (2001). Modulation of recombinant small-conductance Ca^{2+}-activated K^+ channels by the muscle relaxant chlorzoxazone and structurally related compounds. *J Pharmacol Exp Ther* **296**: 683–689.

Cao YJ, Dreixler JC, Couey JJ, Houamed KM (2002). Modulation of recombinant and native neuronal SK channels by the neuroprotective drug riluzole. *Eur J Pharmacol* **449**: 47–54.

Carignani C, Roncarati R, Rimini R, Terstappen GC (2002). Pharmacological and molecular characterisation of SK3 channels in the TE671 human medulloblastoma cell line. *Brain Res* **939**: 11–18.

Cingolani LA, Gymnopoulos M, Boccaccio A, Stocker M, Pedarzani P (2002). Developmental regulation of small conductance Ca^{2+}-activated K^+ channel expression and function of rat purkinje neurons. *J Neurosci* **22**: 4456–4467.

Devor DC, Singh AK, Frizzell RA, Bridges RJ (1996). Modulation of Cl^- secretion by benzimidazolones. I. Direct activation of a Ca^{2+}-dependent K^+ channel. *Am J Physiol* **271**: L775–L784.

Eichler I, Wibawa J, Grgic I, Knorr A, Brakemeier S, Pries AR *et al*. (2003). Selective blockade of endothelial Ca^{2+}-activated small- and intermediate-conductance K^+-channels suppresses EDHF-mediated vasodilation. *Br J Pharmacol* **138**: 594–601.

Faber ESL, Sah P (2002). Physiological role of calcium-activated potassium currents in the rat lateral amygdala. *J Neurosci* **22**: 1618–1628.

Gu N, Vervaeke K, Hu H, Storm JF (2005). Kv7/KCNQ/M and HCN/h, but not $K_{Ca}2$/SK channels, contribute to the somatic medium after-hyperpolarization and excitability control in CA1 hippocampal pyramidal cells. *J Physiol* **566**: 689–715.

Ishii TM, Silvia C, Hirschberg B, Bond CT, Adelman JP, Maylie J (1997). A human intermediate conductance calcium-activated potassium channel. *Proc Natl Acad Sci USA* **94**: 11651–11656.

Jensen BS, Strøbæk D, Christophersen P, Jørgensen TD, Hansen C, Silahtaroglu A *et al*. (1998). Characterization of the cloned human intermediate-conductance Ca^{2+}-activated K^+ channel. *Am J Physiol* **275**: C848–C856.

Ji H, Shepard PD (2006). SK Ca^{2+}-activated K^+ channel ligands alter the firing properties of dopamine-containing neurons *in vivo*. *Neuroscience* **140**: 622–633.

Khanna R, Chang MC, Joiner WJ, Kaczmarek LK, Schlichter LC (1999). hSK4/hIK1, a calmodulin-binding KCa channel in human T lymphocytes. Roles in proliferation and volume regulation. *J Biol Chem* **274**: 14838–14849.

Kohler M, Hirschberg B, Bond CT, Kinzie JM, Marrion NV, Maylie J *et al*. (1996). Small-conductance, calcium-activated potassium channels from mammalian brain. *Science* **273**: 1709–1714.

Lappin SC, Dale TJ, Brown JT, Trezise DJ, Davies CH (2005). Activation of SK channels inhibits epileptiform bursting in hippocampal CA3 neurons. *Brain Res* **1065**: 37–46.

LeMasurier M, Heginbotham L, Miller C (2001). It's a potassium channel. *J Gen Physiol* **118**: 303–313.

Matthews RT, McMillen BA, Speciale SG, Jarrah H, Shore PA, Sanghera MK *et al*. (1984). Effects of zoxazolamine and related centrally acting muscle relaxants on nigrostriatal dopaminergic neurons. *Brain Res Bull* **12**: 479–486.

Pedarzani P, Mosbacher J, Rivard A, Cingolani LA, Oliver D, Stocker M *et al*. (2001). Control of electrical activity in central neurons by modulating the gating of small conductance Ca^{2+}-activated K^+ channels. *J Biol Chem* **276**: 9762–9769.

Pedarzani P, McCutcheon JE, Rogge G, Jensen BS, Christophersen P, Hougaard C *et al*. (2005). Specific enhancement of SK channel activity selectively potentiates the after hyperpolarizing current I(AHP) and modulates the firing properties of hippocampal pyramidal neurons. *J Biol Chem* **280**: 41404–41411.

Pedersen KA, Schrøder RL, Skaaning-Jensen B, Strøbæk D, Olesen SP, Christophersen P (1999). Activation of the human intermediate-conductance Ca^{2+}-activated K^+ channel by 1-ethyl-2-benzimidazolinone is strongly Ca^{2+}-dependent. *Biochim Biophys Acta* **1420**: 331–340.

Sailer CA, Kaufmann WA, Marksteiner J, Knaus HG (2004). Comparative immunohistochemical distribution of three small-conductance Ca^{2+}-activated potassium channel subunits, SK1, SK2, and SK3 in mouse brain. *Mol Cell Neurosci* **26**: 458–469.

Sauvé R, Simoneau C, Monette R, Roy G (1986). Single-channel analysis of the potassium permeability in HeLa cancer cells: evidence for a calcium-activated potassium channel of small unitary conductance. *J Membr Biol* **92**: 269–282.

Schumacher MA, Rivard AF, Bachinger HP, Adelman JP (2001). Structure of the gating domain of a Ca^{2+}-activated K^+ channel complexed with Ca^{2+}/calmodulin. *Nature* **410**: 1120–1124.

Shepard PD, Bunney BS (1988). Effects of apamin on the discharge properties of putative dopamine-containing neurons *in vitro*. *Brain Res* **463**: 380–384.

Singh S, Syme CA, Singh AK, Devor DC, Bridges RJ (2001). Benzimidazolone activators of chloride secretion: potential therapeutics for cystic fibrosis and chronic obstructive pulmonary disease. *J Pharmacol Exp Ther* **296**: 600–611.

Stocker M, Pedarzani P (2000). Differential distribution of three Ca^{2+}-activated K^+ channel subunits, SK1, SK2, and SK3, in the adult rat central nervous system. *Mol Cell Neurosci* **15**: 476–493.

Strassmaier T, Bond CT, Sailer CA, Knaus HG, Maylie J, Adelman JP (2005). A novel isoform of SK2 assembles with other SK subunits in mouse brain. *J Biol Chem* **280**: 21231–21236.

Strøbæk D, Hougaard C, Johansen TH, Sørensen US, Nielsen EØ, Nielsen KS *et al*. (2006). Inhibitory gating modulation of small conductance Ca^{2+}-activated K^+ channels by the synthetic compound *(R)-N*-(Benzimidazol-2-yl)-1,2,3,4-tetrahydro-1-naphtylamine (NS8593) reduces afterhyperpolarizing current in hippocampal CA1 neurons. *Mol Pharmacol* **70**: 1–12.

Strøbæk D, Jørgensen TD, Christophersen P, Ahring PK, Olesen SP (2000). Pharmacological characterization of small-conductance Ca^{2+}-activated K^+ channels stably expressed in HEK 293 cells. *Br J Pharmacol* **129**: 991–999.

Strøbæk D, Teuber L, Jørgensen TD, Ahring PK, Kjær K, Hansen RS *et al*. (2004). Activation of human IK and SK Ca^{2+}-activated K^+ channels by NS309 (6,7-dichloro-1H-indole-2,3-dione 3-oxime). *Biochim Biophys Acta* **1665**: 1–5.

Syme CA, Gerlach AC, Singh AK, Devor DC (2000). Pharmacological activation of cloned intermediate- and small-conductance Ca^{2+}-activated K^+ channels. *Am J Physiol* **278**: C570–C581.

Walter JT, Alvina K, Womack MD, Chevez C, Khodakhah K (2006). Decreases in the precision of Purkinje cell pacemaking cause cerebellar dysfunction and ataxia. *Nat Neurosci* **9**: 389–397.

Waroux O, Massotte L, Alleva L, Graulich A, Thomas E, Liégeois JF *et al*. (2005). SK channels control the firing pattern of midbrain dopaminergic neurons *in vivo*. *Eur J Neurosci* **22**: 3111–3121.

Weaver CD, Harden D, Dworetzky SI, Robertson B, Knox RJ (2004). A thallium-sensitive, fluorescence-based assay for detecting and characterizing potassium channel modulators in mammalian cells. *J Biomol Screen* **9**: 671–677.

Wolfart J, Neuhoff H, Franz O, Roeper J (2001). Differential expression of the small-conductance, calcium-activated potassium channel SK3 is critical for pacemaker control in dopaminergic midbrain neurons. *J Neurosci* **21**: 3443–3456.

Xia XM, Fakler B, Rivard A, Wayman G, Johnson-Pais T, Keen JE *et al*. (1998). Mechanism of calcium gating in small-conductance calcium-activated potassium channels. *Nature* **395**: 503–507.